Method for Designing Closed Airfoils for Arbitrary Supercritical Speed Distributions

G. Volpe* and R. E. Melnik†
Grumman Corporate Research Center, Bethpage, New York

A method for designing airfoil profiles of specified trailing-edge thickness corresponding to given arbitrary supercritical speed distributions is described in this paper. It is known that the surface speed must satisfy three constraints in order for a solution to exist. Hence, to guarantee satisfaction of the constraints in our method, the speed distribution is specified with three free parameters whose values are found automatically. The modifications introduced to an ideal target speed distribution are everywhere smooth and avoid the occasional "spikes" that were present in an earlier version of the method. The new functional forms used to modify the ideal target are well behaved at all times and prevent undue excursions of the airfoil profile during the iteration process. As a result, the iteration is much faster than in the earlier version of the method and it is now possible to quickly design airfoil shapes that are shockless or have shocks on the surface or off in the field.

Introduction

AIRFOIL sections for supercritical applications can be designed numerically in a number of different ways, with each approach having its particular advantages and disadvantages. In the early 1970s hodograph methods such as those of Garabedian and Korn (described in Ref. 1) and Boerstoel and Muizing[2] were formulated and used to generate a number of contours. Hodograph methods are extremely difficult to use, however, since the data input needed is not easily identifiable with the physical or flow characteristics required of the airfoil to be designed.

With the development of reliable algorithms for calculating the flow over known airfoil shapes, a second class of "direct" methods, far easier to use, came into being. By comparing the solution (pressure distribution and/or force characteristics) for the flow over some arbitrary initial airfoil contour with a desired pressure distribution or force coefficients, the contour is modified in some rational way in the hope of reducing the differences between the "target" and the "current" characteristics. The process obviously has to be iterated. This is the approach followed by Hicks et al.,[3] Davis,[4] and McFadden.[5] The methods of Tranen[6] and Carlson[7] also belong in this category since they are not correctly formulated as inverse methods. One advantage of the "direct-type" methods is that a realistic airfoil shape can be retained at every step of the iteration. Its biggest disadvantage, however, is the lack of a guarantee that the iteration will converge with differences between computed and target values reduced to arbitrarily small levels.

An alternative approach is to use an inverse method in which the airfoil contour is generated through the solution of a Dirichlet problem whose boundary conditions are set by the "target" speed distribution. This type of inverse method has been employed for incompressible and subsonic airfoil design by Mangler,[8] Lighthill,[9] Woods,[10] Van Ingen,[11] Arlinger,[12] and Strand.[13] The main obstacle to the design of airfoils by this approach arises from the fact that the inverse problem will generally not have a solution unless the prescribed speed distribution satisfies three constraints. This has been shown clearly by Mangler[8] and Lighthill.[9] One constraint requires that the target speed distribution on the airfoil surface be compatible with the prescribed freestream speed. Two additional constraints arise from the requirement that the airfoil be closed (or have a specified gap at the trailing edge). The constraints were formulated in integral form by Mangler and Lighthill for incompressible flow and by Woods[10] for compressible subcritical flow of a Karman-Tsien type of gas. If the target speed distribution satisfies the three constraints, then a solution to the inverse problem will always exist. Thus, in the applications carried out in Refs. 11-13, the target speed distribution was specified with three free parameters whose values were adjusted to satisfy the three integral constraints. In these methods, the introduction of the free parameters could be arranged such that the "ideal" speed distribution was modified only over selected segments of the airfoil surface. Desired characteristics of the speed distribution (e.g., "rooftops," Stratford-type pressure recovery, rear or front loading) could be retained without modification if needed.

Difficulties existed in formulating an inverse method for transonic speeds since the three constraints on the target speed distribution could no longer be expressed in closed form. The lack of a clear understanding of the first constraint was the main source of the difficulties. Volpe and Melnik[14] recognized that the first constraint could be satisfied by treating the value of the freestream speed as a free parameter that is determined as part of the solution of the Dirichlet problem. Alternatively, the target surface speed distribution could be scaled keeping the freestream speed fixed. These two options are equivalent in practice, since the quantity of interest is the ratio of the surface-to-freestream speed. A method for designing airfoils without any control of the trailing-edge gap was described in Ref. 14. The airfoils designed by that method were open at the trailing edge because the additional pair of constraints on the trailing edge was not enforced.

Later, Volpe[15] employed the method of Ref. 14 to determine the sensitivity of the computed freestream speed and trailing-edge gap to various classes of target surface speed distributions. These results were later used to develop an iterative procedure to design airfoils with closed trailing edges. In the new method,[16] three free parameters are adjusted numerically to drive the values of the freestream speed and trailing-edge gap dimensions to prescribed values. The parameters were introduced in such a way that each mainly affected only one of the constraints. This permitted the formulation of

Presented as Paper 85-5023 at the AIAA 3rd Applied Aerodynamics Conference, Colorado Springs, CO, Oct. 14-16, 1985; received Nov. 4, 1985; revision received April 8, 1986.

*Staff Scientist, Theoretical Aerodynamics. Member AIAA.
†Director, Fluid Mechanics. Member AIAA.

a diagonal-type iterative scheme in which the three parameters could be determined from three uncoupled one-dimensional relaxation methods. The introduction of the three free parameters into the target speed distribution led to a robust method for the design of airfoils that generated a close approximation to a prescribed ideal. Unfortunately, the method described in Ref. 16 occasionally generated airfoils with spikes in the resulting pressure distribution near leading edges.

In this paper, we describe an improved scheme for introducing the necessary freedom into the target speed distribution that completely eliminates the undesirable spikes from the solution. As an added benefit, we found that the elimination of leading-edge spikes also significantly improved the convergence of the method.

Formulation of the Design Problem

The problem we consider is that of constructing the airfoil profile that will have a surface speed distribution q_0 equal to some desired function $F_0(s)$ everywhere along its arc length. We also specify the freestream uniquely by defining values for the freestream velocity, temperature, and pressure (or density). These in turn determine the freestream Mach number. In incompressible flow, of course, we need specify only the velocity to identify the freestream uniquely. Our formulation applies in its entirety if we specify a surface pressure distribution instead of a surface speed, since the two are uniquely related. As discussed previously, this problem generally does not have a solution unless the prescribed speed distribution contains several free parameters. These arise from the requirement that the upper and lower surface trailing-edge points be separated by prescribed distances δx and δy. The horizontal gap δx is always set to zero in all cases, while the vertical gap δy is either set to zero (a closed airfoil) or to a small positive number. An additional requirement is that the solution in the far field approaches a uniform freestream plus a circulatory component as discussed by Ludford.[17] These requirements are easily overlooked as evidenced by the formulations of the airfoil design codes of Tranen[6] and Carlson.[7] The magnitude of the circulation term in the far field is given by the lift implied by the prescribed function $F_0(s)$. Less well known is the fact that the prescribed surface speed $q_0 = F_0(s)$ also determines the magnitude of the freestream speed. This is easily demonstrated for incompressible nonlifting flow over a circle, since in such a case the most general expression for the velocity at any point in the flowfield is of the form

$$q = q_\infty - \sum_{n=2}^{\infty} b_n \zeta^{-n} \tag{1}$$

where q_∞ is the magnitude of the freestream speed, $\zeta = re^{i\omega}$ the polar coordinates of the plane, and b_n constants. If we specify $q = q_0$ on a unit circle ($r = 1$), we can expand q_0 in a Fourier series

$$q_0(\omega) = c_0 + \sum_{n=1}^{N} c_n e^{-in\omega} \tag{2}$$

At $\zeta = 1$, Eqs. (1) and (2) must be identical. The b_n in Eq. (1) can thus be computed and we notice that the value of the freestream q_∞ must also be equal to the zero order term in q_0. This was Lighthill's first and Mangler's third constraint in their formulation of the airfoil design problem. The absence of first-order terms in Eq. (1) leads to two additional constraints corresponding to the trailing-edge gap requirements. Detailed discussions of the three constraints can be found in Refs. 8 and 9 for incompressible flow and Refs. 14 and 16 for transonic flow.

As a consequence of the constraints, an airfoil of trailing-edge gap dimensions (δx, δy) corresponding to a speed distribution $F_0(s)$ exists only if F_0 contains three free parameters. Two of these parameters are adjusted to give the desired δx and δy. The third is adjusted so that the target surface speed distribution is compatible with the specific freestream speed. The most general speed distribution we can specify is, therefore,

$$q_0/q_\infty = F_0(s;p_1,p_2,p_3) \tag{3}$$

where p_1, p_2, and p_3 are the three adjustable parameters whose values are to be found together with the airfoil solution. In this paper, we assume the speed distribution to be of the form

$$q_0/q_\infty = f_1(s;p_1)[f_0(s) + f_2(s;p_2) + f_3(s;p_3)] \tag{4}$$

where $f_0(s)$ represents the "ideal" target speed distribution that, in practice, is usually a tabulated function. f_1, f_2, and f_3 are specified functions that modify the ideal target in order to satisfy the three constraints. In general, it is desirable to localize the effect of f_1, f_2, and f_3 so that the resulting surface speed will be close to the ideal speed distribution $f_0(s)$ over most of the airfoil surface. Since in transonic flow it is not

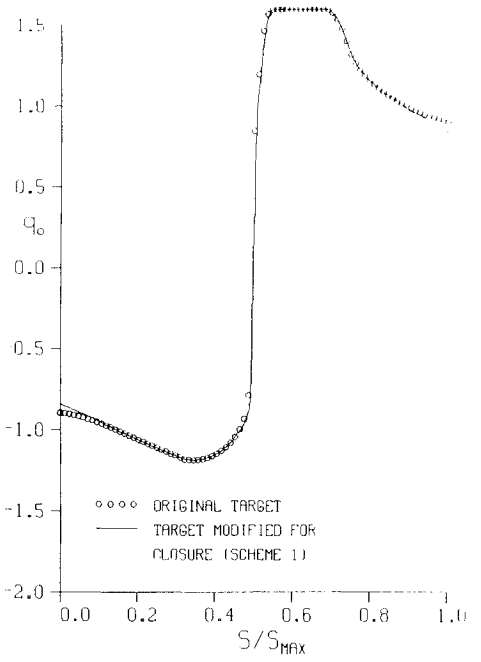

Fig. 1 Original and modified target speed distributions: "shockless" case, $M_\infty = 0.800$, $\alpha = 0$ deg.

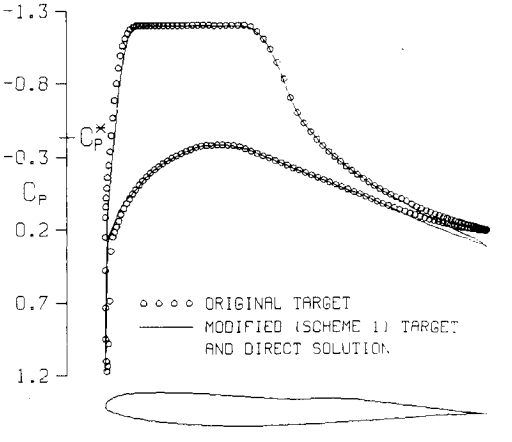

Fig. 2 Designed contour, original target, and computed pressure distribution: "shockless" case, $M_\infty = 0.800$, $\alpha = 0$ deg, $C_L = 0.4801$, $C_D = 0.0232$.

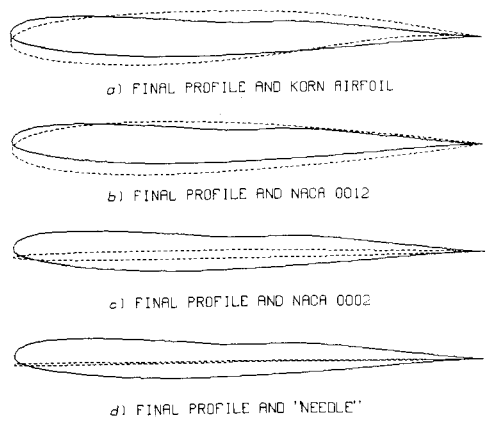

Fig. 3 Final airfoil profile (solid line) compared with starting profile (dashed line).

possible to relate p_1, p_2, and p_3 to the three constraints in closed form, a numerical search for the parameters must be made. The search is greatly facilitated by choosing f_1, f_2, and f_3 in such a way that each significantly affects only one of the constraints. We would then have three one-dimensional searches for p_1, p_2, and p_3. The airfoil design sensitivity studies of Volpe[15] enable us to do this.

Satisfaction of the first constraint is guaranteed by adjustment of p_1. f_1 by definition causes a scaling of surface speed (q_0/q_∞). By choosing $f_1 = p_1$, the scaling is made uniform along the airfoil. In such a case, we could consider p_1 as a scaling on either q_0 or q_∞. In the latter case, we would essentially have q_∞ floating and it would be determined as part of the solution. The scaling can be concentrated in the front half of the airfoil by choosing

$$f_1 = \sqrt{1 + p_1 \sin^2(\omega/2)} \tag{5}$$

Here we are substituting the ordinate ω in the computational plane for the arc length s. All our computations are carried out in the computational plane obtained by mapping the airfoil (any airfoil) into the unit circle. The ordinate ω (running from zero to 2π) then identifies the length along the airfoil surface from the trailing-edge point on the lower surface to the corresponding point on the upper surface. It is more convenient to use ω rather than s and the formulation of the problem is not affected by this substitution.

Control over δy, the separation between the upper and lower surface trailing-edge points, can be exercised by defining

$$f_2 = p_2 \sin\left(\frac{8}{3}\omega\right), \qquad \omega \le \frac{3}{4}\pi \tag{6}$$

Outside this range, f_2 is zero. This function alters the target speed distribution only on the lower surface of the airfoil. It would, therefore, be unsatisfactory if we were trying to design a symmetric airfoil. An alternative form for f_2 is

$$f_2 = p_2\left(1 - \frac{\omega}{\omega_1}\right), \qquad \omega \le \omega_1$$

$$= p_2\left(\frac{2\pi - \omega}{\omega_1} - 1\right), \qquad \omega \ge 2\pi - \omega_1 \tag{7}$$

This function symmetrically alters the magnitude of the speed in the neighborhood of the trailing edge. In our computational scheme, the speed takes on opposite signs on the upper and lower surfaces, accounting for the sign difference between the two parts of Eq. (7). ω_1 is typically taken as $\pi/3$.

The horizontal separation δx between the two trailing-edge points is affected primarily by the location of the leading-edge stagnation point. As shown in Ref. 15, a small shift in this

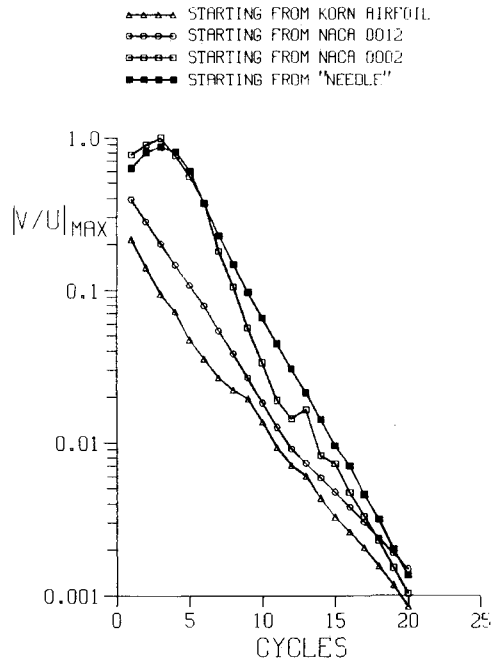

Fig. 4 Convergence history of maximum surface velocity ratio for various starter profiles: "shockless" case, $M_\infty = 0.800$, $\alpha = 0$ deg.

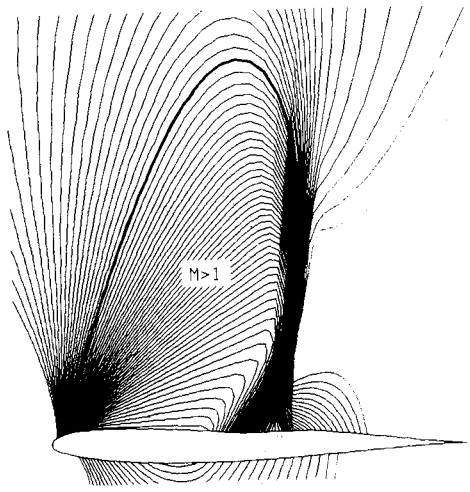

Fig. 5 Design point isomachs: "shockless" case, $M_\infty = 0.800$, $\alpha = 0$ deg (contours shown at 0.01 intervals beginning with $M = 0.810$).

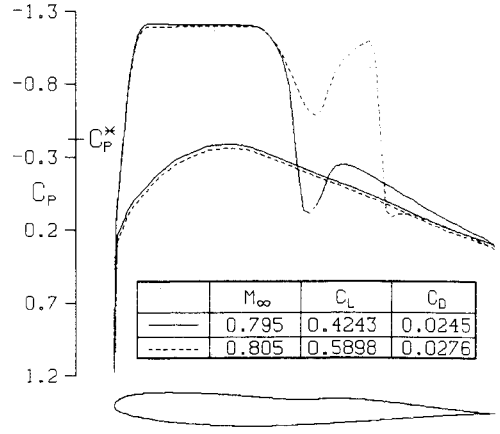

Fig. 6 Off-design analysis of "shockless" case, $\alpha = 0$ deg (C_p^* corresponds to $M_\infty = 0.795$).

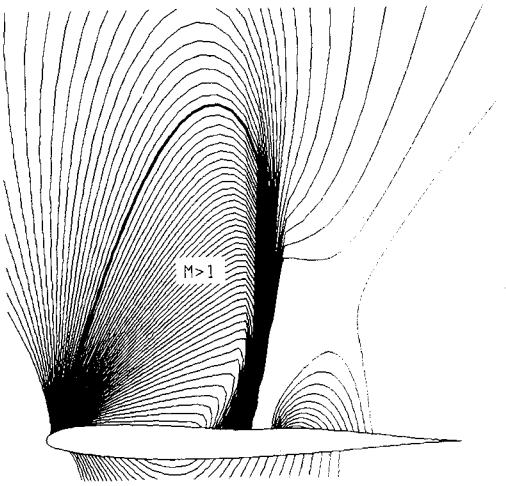

Fig. 7 Off-design isomachs: "shockless" case, $M_\infty = 0.795$, $\alpha = 0$ deg, (contours shown at 0.01 intervals beginning with $M = 0.810$).

stagnation point along the surface of the airfoil, on the order of 2% of the chord length, can alter the horizontal gap by 5-6%. It should be pointed out that a shift in the stagnation point of 2% along the surface is hardly noticeable when viewed as a shift along the chord. In order to maintain a loose coupling among p_1, p_2, and p_3, the shift must be accomplished without altering the local velocity gradients. In the method described in Ref. 16, a function was proposed for f_3 that served the purpose. However, spikes were occasionally introduced in the target distribution near the points where f_3 returned to zero. A much better strategy is to shift the functional dependence of q_0 on s locally near the leading edge. Thus, we let

$$f_3(s) = f_0(s') - f_0(s) \tag{8}$$

with

$$s' = s - p_3 h(s) \tag{9}$$

where

$$h(s) = \frac{1}{2}\left\{1 - \cos\left[\frac{\pi}{\Delta s}(s - s_T + 2\Delta s)\right]\right\}, \quad s_T - 2\Delta s \le s \le s_T - \Delta s$$

$$= 1, \quad s_T - \Delta s \le s \le s_T + \Delta s$$

$$= \frac{1}{2}\left\{1 + \cos\left[\frac{\pi}{\Delta s}(s - s_T + \Delta s)\right]\right\}, \quad s_T + \Delta s \le s \le s_T + 2\Delta s \tag{10}$$

Elsewhere $h(s)$ is zero. s_T is the point where $f_0(s)$ is zero in the leading-edge region and Δs is some appropriate distance, typically 2.5% of the total arc length. This form for f_3 shifts the leading-edge stagnation point smoothly without introducing any wiggles in the target speed distribution and, in addition, has hardly any effect on the values of p_1 and p_2.

Airfoil Design Scheme

The airfoil corresponding to the target speed distribution represented by Eq. (4) in which $f_0(s)$ represents the "ideal" target is obtained by iteratively modifying some initial contour. This initial contour need not be "close" to the sought-after profile for the iteration to converge. The scheme for modifying the airfoil is the scheme first described by Volpe and Melnik[14] and, in brief, it proceeds as follows. The initial contour is mapped into the unit circle by a transformation of the form

$$\frac{dz}{d\zeta} = \left(1 - \frac{1}{\zeta}\right)^{(1-\epsilon)} e^{P+iQ} \tag{11}$$

where $z = x + iy$ and $\zeta = re^{i\omega}$ are the coordinates in the physical and mapped planes, respectively, and $\epsilon\pi$ is the included trailing-edge angle. Separating this expression into its real and imaginary parts, we obtain (for $r = 1$)

$$\frac{ds}{d\omega} = \left(2 \sin\frac{\omega}{2}\right)^{(1-\epsilon)} e^{P} \tag{12}$$

$$\theta = \frac{1}{2}(1+\epsilon)(\pi - \omega) - \frac{\pi}{2} + Q \tag{13}$$

where θ is the local slope of the airfoil. Q is the Fourier series

$$Q = \sum_{n=0}^{N} (A_n \sin n\omega - B_n \cos n\omega) \tag{14}$$

and P is its conjugate series. As described in Ref. 10, if θ is known as a function of s, the coefficients of the series are found by a standard Fourier analysis of Eq. (13). In this mapping, the first-order terms of the series are related to the trailing-edge gap dimensions by

$$A_1 = g_1(\delta x, \delta y; B_0, \epsilon), \qquad B_1 = g_2(\delta x, \delta y; B_0, \epsilon) \tag{15}$$

where g_1 and g_2 represent bilinear functions in δx and δy. Having mapped the airfoil to a circle and the physical plane outside the airfoil to the inside of the circle, the next step is the solution of the appropriate flow equations subject to the Dirichlet boundary conditions that the tangential speed on the circle, u, be equal to the total target speed q_0 to which we are designing the airfoil. For incompressible flow, the flow is described by Laplace's equation, and the solution can be expressed in closed form. For transonic flow, the solution must be determined numerically, whether we assume the flow to be described by the potential equation, as we do here, or by a set of Euler equations. Regardless of which equations are assumed to describe the flowfield, in this Dirichlet-type problem the circle boundary (as well as the initial airfoil contour) is not necessarily a streamline and the component of velocity normal to the circle, v, will not be zero, in general. If the boundary represented the airfoil corresponding to the specified q_0, then $v = 0$ and this will be true at the convergence of our iterative procedure. At intermediate stages a nonzero v implies that the actual streamline is (to first order) at incidence from the assumed boundary by an angle of magnitude

$$\delta\theta = \tan^{-1}(v/u) \tag{16}$$

Equation (16) is used to modify the initial slope distribution θ in Eq. (13). New Fourier series for Q and P can be computed as well as a new $ds/d\omega$ and

$$\frac{dx}{d\omega} = -\frac{ds}{d\omega}\cos\theta, \qquad \frac{dy}{d\omega} = -\frac{ds}{d\omega}\sin\theta \tag{17}$$

s, x, and y are then obtained by integration. Using this new airfoil shape, a new Dirichlet problem can be set up and the process is iterated until a desired tolerance for $|v/u|$ is achieved. During the iteration procedure p_2 and p_3 in Eq. (4) are adjusted in order that the airfoil will have the desired trailing-edge dimensions.

We must notice from Eq. (16) that our contour modification procedure fails at points where $u = 0$ unless v is also zero there. In our method, we force v to be zero at the leading-edge point where u (and q_0) are specified to be zero. This is ac-

complished by adjusting p_1. In incompressible flow, it has been shown that with this procedure the first constraint is satisfied. Details can be found in Refs. 14 and 16. In contrast to the problem in which the total velocity distribution $q_0 = f_0(s)$ is specified on the boundary and that gives rise to the first constraint, at any stage of our numerical procedure only the tangential velocity $u = f_0(s)$ on the boundary is specified. For incompressible flow, it can be shown quite easily that in this latter case the freestream speed can also be specified simultaneously without setting up any incompatibilities between the two boundaries. For each q_∞ we pick (for a fixed p_1 on the circle boundary) or for each p_1 we pick on the boundary (for fixed q_∞), we set up flows that have different v distributions on the circle boundary. In each of these incompressible flows, the airfoil-type contours containing a branch point, and on which a speed distribution is some multiple of $f_0(s)$, are identical except for a scale factor and a translation. Details can be found in Ref. 16. In each of these flows, the airfoil-like contour could be found by first locating the branch point (leading-edge stagnation point) and then following the two departing streamlines. Placing the branch point at a known position (where $u = 0$ on the circle boundary) makes the determination of the contour more convenient without introducing any restrictions. This procedure automatically satisfies the first constraint in incompressible flow and, in addition, for the case where $f_1 = p_1$ in Eq. (4), the scaling factor p_1 is identical to that found by enforcing Lighthill's first integral constraint.[9] In contrast to the integral constraints, this procedure can be applied to compressible supercritical flows.

Briefly, then, in our procedure during the inner iteration for the solution of the flowfield, we let q_∞ float and pick for q_∞ the value that forces v to be zero at the leading-edge point where u (as well as q_0) is specified to be zero. Then, p_1 in Eq. (4) is adjusted to scale the target speed in order to restore q_∞ to its initially prescribed value. As a result of this procedure, $\delta\theta$ in Eq. (16) will always be finite and the first constraint will be satisfied for all f_0 and any q_∞.

The solution to the Dirichlet problem, in general, entails a nonzero net mass flow through the boundary. As shown by Ludford,[17] the correct far-field boundary conditions must then contain a mass flow term σ. The value of this term can be computed by enforcing the condition that v be zero at the trailing edge of the airfoil. This is analogous to the condition for evaluating the circulation in the direct Neumann problem for the airfoil where u is forced to be finite at the trailing edge. Thus, in practice, q_∞ and σ are evaluated simultaneously by forcing v to be zero at the leading- and trailing-edge stagnation points. As the contour iteration converges to the airfoil, σ goes to zero, as shown in Ref. 14.

In the present method, we assume the flow to be described by the full potential equation, which is solved by a numerical algorithm first developed by Jameson[18] for the Neumann problem. The scheme relies on an alternating direction implicit (ADI) recursion with multigrid sequencing of the meshes to accelerate convergence. The full potential equation is discretized in full conservative form on a polar coordinate grid within the unit circle that represents the boundary. The speed distribution in Eq. (4), the target, is integrated to give the surface boundary conditions. The far-field boundary conditions must contain freestream, mass flow, and circulation terms, as shown by Ludford.[17] The solution of each Dirichlet problem is then obtained as follows. The flowfield is swept once on each grid down and back through the meshes up to the basic working mesh. At this point, q_∞ and σ are determined by forcing v to be zero at the leading-edge point where u is zero and at the trailing edge. p_1 is then adjusted to scale q_∞ back to its specified value and the flowfield is swept again. v at the leading-edge stagnation point goes to zero quite fast (due to the continuous resetting of p_1). When v is below a given tolerance (typically 10^{-5}–10^{-6}), estimates are made of the values that A_1 and B_1, the first-order terms of the series in Eq. (14), would have if the airfoil were to be modified at that stage. These values are compared with the values they should have for the airfoil to have the desired trailing-edge gap dimensions, as given by Eq. (15). The differences between the current and desired values, δA_1 and δB_1, are then used to change p_2 and p_3, respectively. The change in p_2 is made proportional to δA_1 and the change in p_3 is proportional to $(-\delta B_1)$. Since p_1 is introduced as a multiplier, a change in the

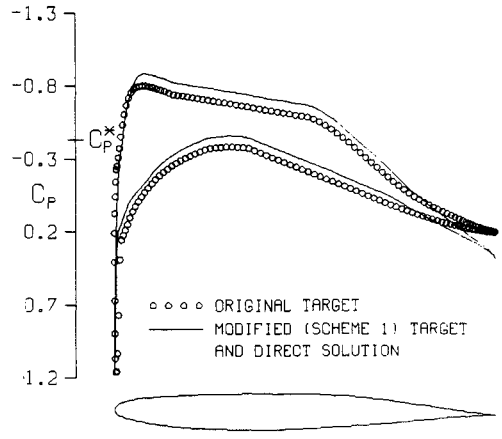

Fig. 9 Designed contour, original target, and computed pressure distribution: case 2a, $M_\infty = 0.800$, $\alpha = 0$ deg, $C_L = 0.3121$, $C_D = 0.0005$.

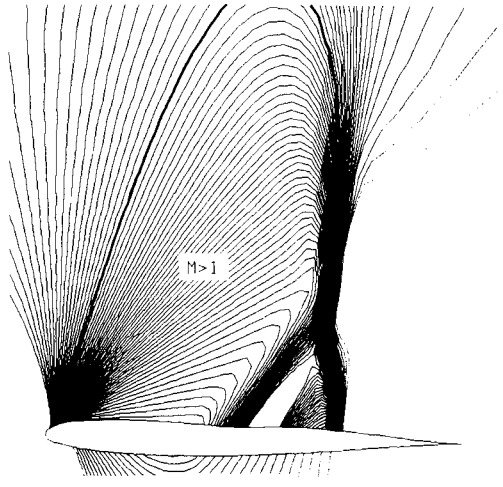

Fig. 8 Off-design isomachs: "shockless" case, $M_\infty = 0.805$, $\alpha = 0$ deg (contours shown at 0.01 intervals beginning with $M = 0.810$).

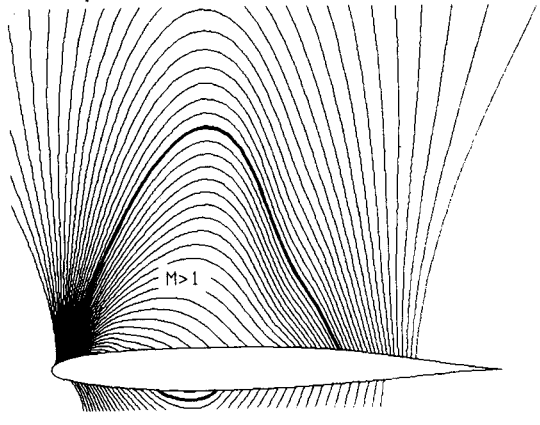

Fig. 10 Design point isomachs: case 2a, $M_\infty = 0.800$, $\alpha = 0$ deg, (contours shown at 0.01 intervals beginning with $M = 0.810$).

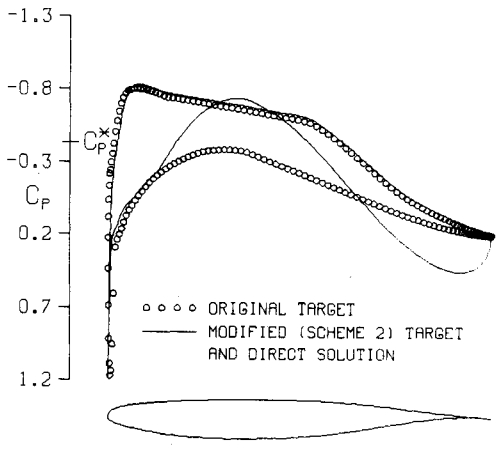

Fig. 11 Designed contour, original target, and computed pressure distribution: case 2b, $M_\infty = 0.800$, $\alpha = 0$ deg, $C_L = 0.2673$, $C_D = 0.0005$.

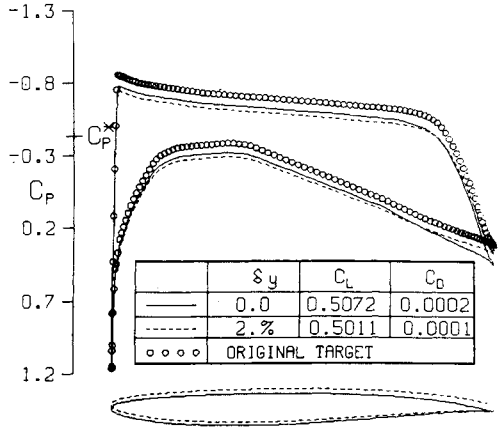

Fig. 13 Original target, computed pressure distributions and contours designed via scheme 1 for $\delta y = 0$ and $\delta y = 2\%$: case 3, $M_\infty = 0.800$, $\alpha = 0$ deg.

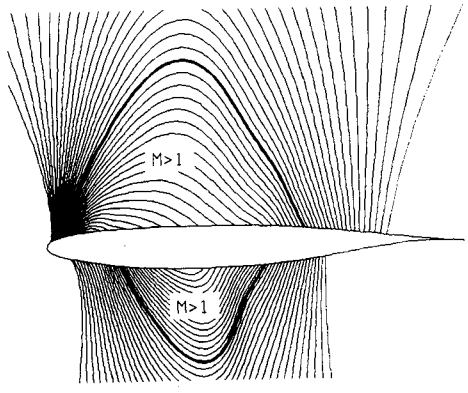

Fig. 12 Design point isomachs: case 2b, $M_\infty = 0.800$, $\alpha = 0$ deg (contours shown at 0.01 intervals beginning with $M = 0.810$).

surface boundary conditions due to a new p_1 can be transmitted through the entire flowfield by scaling the entire potential field. Using this procedure, we can update p_1 after each multigrid sweep of the flowfield without seriously affecting the convergence rate of the numerical scheme. This procedure is not possible with p_2 and p_3 and, therefore, they are updated only infrequently. However, the method of false position can be used to accelerate convergence of p_2 and p_3. The flowfield is assumed to be converged when all the residuals at all the flowfield node points are below a specified tolerance and v at the leading-edge stagnation point together with δA_1 and δB_1 are below their respective tolerances. At this point, the airfoil contour is modified and another Dirichlet problem is set up. There is no need to analyze the new airfoil contour with this procedure. A direct analysis is made at the very end of the calculation just to check our results.

Results

The method has been used to design a very large number of airfoils over a wide range of speed (or pressure) distributions with and without shock waves. A few examples will be presented here, all at a freestream Mach number of 0.80 and zero angle of attack. In our formulation, we are free to specify the angle of attack. Different choices for the angle of attack result in different orientations of an otherwise identical contour. All our calculations have been carried out on a grid containing 192 points in the circumferential directions by 32 in the radial direction with 5 mesh levels in the multigrid sequence.

The symbols in Fig. 1 depict a speed distribution for which a closed (zero trailing edge gap) airfoil is sought. This distribution represents the function $f_0(s)$ in Eq. (4). In order to satisfy the three constraints, it must be modified into the distribution depicted by the solid line. The modification is achieved by taking f_1 to be a constant (as will be the case in the remaining examples except as noted), f_2 to be as given by Eq. (7), and f_3 as defined in Eqs. (8-10). We call this strategy for modifying the speed distribution scheme 1. The required values of the associated parameters p_1, p_2, and p_3 are found automatically by the program as part of the airfoil solution. The shift in the location of the stagnation point should be noticed in Fig. 1. The shift is achieved smoothly and makes it possible to close the x gap in the airfoil. The designed airfoil is depicted in Fig. 2 along with the computed pressure distribution. This pressure distribution is the result of a direct solution of the flowfield over the designed airfoil contour and it agrees to three decimal places with the pressure distribution that corresponds to the target speed distribution (the solid line in Fig. 1). This airfoil solution is obtained regardless of the airfoil contour initially prescribed to start the iteration procedure. In Fig. 3 the designed airfoil contour is compared with four different starting shapes: the Korn airfoil, the NACA 0012, the NACA 0002, and, finally, a "needle" (two straight lines joined at the trailing edge and at the leading edge tangent to a semicircle of radius equal to 0.25% of the chord).

It is satisfying to note that the values of p_1, p_2, and p_3 are identical regardless of the starting shape (i.e., the modified target speed distribution is the same in all cases). Apparently, by decoupling the three parameters, we have assured that there exists only a single set of values that satisfies the three constraints. It is possible that if the three parameters had been coupled, more than one set of values might exist that would satisfy the constraints. Even though we have no formal proof of this, decoupling appears to guarantee a unique solution, besides making the search simpler and, therefore, faster. A measure of the convergence rate of the method is given in Fig. 4, which depicts the maximum value of $|v/u|$ as a function of design cycles. Usually, after 10-12 cycles, it is difficult to distinguish any changes in the airfoil shape. Thus, reducing the maximum $|v/u|$ to 0.05 essentially denotes convergence. Typically, we run the code to a level where the maximum $|v/u|$ is 0.001 or smaller.

The pressure distribution depicted in Fig. 2 appears to have very desirable features; in particular, the "plateau" region on the upper surface suggests the absence of a shock. However, a very large drag ($C_D = 0.0232$) is present even at the design point. If we look at the Mach number contours in Fig. 5, we see that, while there is no shock at the airfoil surface itself, a very strong shock is present off the surface. The contours represent increments of 0.01 in Mach number and only contours for values greater than the freestream are shown. At off-design conditions, the shock reaches the surface, as can be

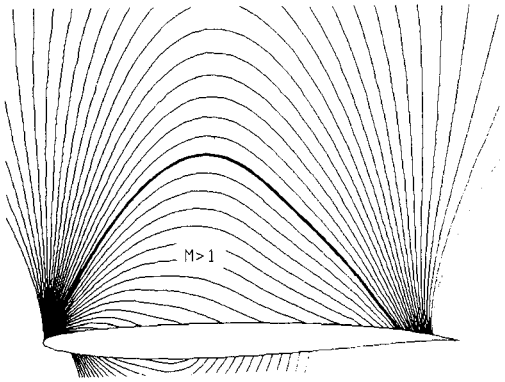

Fig. 14 Design point isomachs: case 3, $\delta y = 0$, $M_\infty = 0.800$, $\alpha = 0$ deg (contours shown at 0.01 intervals beginning with $M = 0.810$).

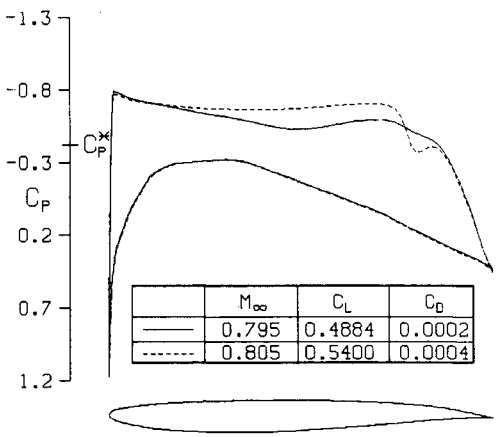

Fig. 15 Off-design analysis of case 3 airfoil ($\delta y = 0$), $\alpha = 0$ deg (C_p^* corresponds to $M_\infty = 0.795$).

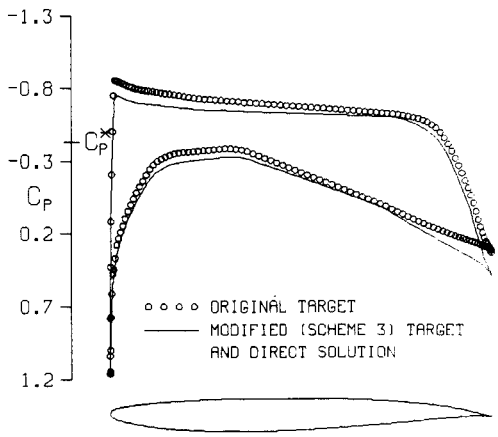

Fig. 16 Designed contour, original target, and computed pressure distribution: case 4, $M_\infty = 0.800$, $\alpha = 0$ deg, $C_L = 0.4972$, $C_D = 0.0002$.

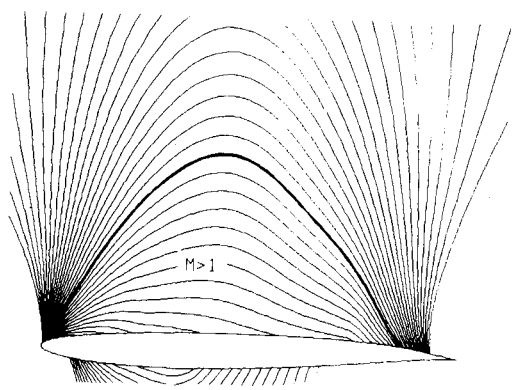

Fig. 17 Design point isomachs: case 4, $M_\infty = 0.800$, $\alpha = 0$ deg, (contours shown at 0.01 intervals beginning with $M = 0.810$).

seen from the pressure distributions in Fig. 6, computed for $M_\infty = 0.795$ and 0.805 and zero angle of attack. The corresponding computed Mach number contours are given in Figs. 7 and 8. Thus, this particular airfoil would be impractical.

A truly shockless closed airfoil is depicted in Fig. 9, along with the computed pressure distribution (i.e., modified target) and the original, unmodified target. Note the low computed drag ($C_D = 0.0005$) of this airfoil. The computed isomach pattern in Fig. 10 shows that the flow over this airfoil is truly shock free and, at off-design points, only a weak shock develops. The scheme for modifying the target speed distribution in this case was the same as the one used in the first example. An alternative strategy for modifying the speed distribution is to choose f_2 to have the form given in Eq. (6) rather than the one given by Eq. (7). We call this scheme 2. This scheme leads to the airfoil depicted in Fig. 11 for the same ideal target. Note that the load distribution of this airfoil is substantially different than in the previous case. As in the previous case, the drag coefficient is very small despite the fact that a substantial pocket of supersonic flow exists on the lower surface, as can be seen from Fig. 12.

The next example in Fig. 13 depicts two airfoils designed to the same ideal target distribution, but with different trailing edge gaps. One is closed and the other has a trailing-edge gap of 2% of the chord in the vertical direction ($\delta y = 2\%$, $\delta x = 0$). The designed airfoil contours for each case are shown along with the corresponding modified target pressure distribution and the ideal target. The modifications were achieved via scheme 1. Both airfoils are shock free as evidenced by the very low drag coefficients. This low drag is achieved in both cases with substantial lift and reasonable airfoil thickness. The isomach contours for the closed airfoil are shown in Fig. 14. At off-design points the performance of these airfoils does not deteriorate quickly. In Fig. 15, the pressure distributions for the closed airfoil at zero angle of attack and freestream Mach numbers of 0.795 and 0.805 are shown. Below the design point, the airfoil is still shock free and, above its design point, a shock develops at a slow rate.

Earlier we mentioned that the scaling introduced by f_1 could be concentrated in the front part of the airfoil by using Eq. (5) rather than a constant f_1. Using the nonuniform scaling together with f_2 given by Eq. (7) (we call this scheme 3), we obtain the airfoil shown in Fig. 16. f_0 in this case in the same distribution as in the previous case. This example should thus be compared with the former. Note that in this case we again obtain a very low drag for the airfoil resulting from the absence of a shock, as can be seen from Fig. 17.

Conclusions

The airfoil design method we have described has proved to be very reliable and fast. By preventing the appearance of unwarranted spikes in the target distribution, a possibility in a previous version of the method, the iteration has been speeded up considerably. A general supercritical speed distribution with or without shock waves can be prescribed and this is modified automatically into one for which an airfoil solution exists. Naturally, shockless airfoils are by far the more interesting and practical cases and, as it has been shown, they can now be generated by a straightforward application of our method. There are no restrictions on the desired trailing-edge gap. A closed trailing edge is only a special case of a very general formulation.

A converged solution ($|v/u| < 0.001$) generally requires 4-5 min of computing time on a Cray-1M machine and about 20 min on an IBM 3081 computer. To achieve engineering accuracy, the design process could be stopped when $|v/u| < 0.05$, which would reduce the running time by approximately 25%. In the latter design cycles, the airfoil shape and the three design parameters are close to their final values. Hence, these cycles need many fewer iterations to converge the flowfield than do the earlier cycles. Thus, the savings that might be expected by increasing the tolerances are not as great as one might expect. If one did not enforce trailing-edge closure, the code would run three or four times as fast as it does in the present mode. In cases where the target speed distribution is only a minor modification of the direct solution over a known airfoil shape, the code could be run in such a manner. For a generally prescribed speed distribution, one could still run the code without enforcing trailing-edge closure and then, at the end of the design process, set the values of first-order terms of the series of the mapping transformation (A_1 and B_1) to the values that give the desired trailing-edge gap. This operation makes subtle changes to the entire airfoil shape. However, in such a case, the differences between the computed pressure distribution and the target will not be necessarily small, especially when the target is a shockless distribution. The code must be run with the first constraint active at all times in order to preserve a well-posed mathematical and numerical problem. As a final comment, it is our feeling that viscous effects can be incorporated into the formulation without noticeably affecting the running time.

References

[1]Bauer, F., Garabedian, P., and Korn, D., *Supercritical Wing Sections*, Springer Verlag, New York, 1972.

[2]Boerstoel, J. W. and Muizing, G. H., "Transonic Shock-Free Airfoil Design by an Analytic Hodograph Method," AIAA Paper 74-439, 1974.

[3]Hicks, R.M., Vanderplaats, G. N., Murman, E. M., and King, R. R., "Airfoil Section Drag Reduction at Transonic Speeds by Numerical Optimization," NASA TMX-73097, Feb. 1976.

[4]Davis, W. M., "Technique for Developing Design Tools from the Analysis Methods of Computational Aerodynamics," AIAA Paper 79-1529, 1979.

[5]McFadden, G. N., "An Artificial Viscosity Method for the Design of Supercritical Airfoils," Courant Institute of Mathematical Sciences, New York University, Res. and Dev. Rept. C00-3077-158, July 1979.

[6]Tranen, T. L., "A Rapid Computer Aided Transonic Airfoil Design Method," AIAA Paper 74-501, 1974.

[7]Carlson, L. A., "Transonic Airfoil Analysis and Design Using Cartesian Coordinates," *Journal of Aircraft*, Vol. 13, 1976, pp. 369-356.

[8]Mangler, W., "Die Berechnung eines Tragflugelprofiles mit Vorgeschriebener Druckverteilung," *Jahrbuch Deutsche Luftfahrtanschung*, 1938.

[9]Lighthill, M. J., "A New Method of Two-Dimensional Aerodynamic Design," British Aeronautical Research Council, R&M 2112, 1945.

[10]Woods, L. C., "Aerofoil Design in Two-Dimensional Subsonic Compressible Flow," British Aeronautical Research Council, R&M 2845, March 1952.

[11]Van Ingen, J. L., "A Program for Airfoil Section Design Utilizing Computer Graphics," *Agard Short Course Notes*, 1969.

[12]Arlinger, B., "An Exact Method of Two-Dimensional Airfoil Design," Saab, Sweden, TN67, 1970.

[13]Strand, T., "Exact Method of Designing Airfoils with Given Velocity Distribution in Incompressible Flow," *Journal of Aircraft*, Vol. 10, 1975, pp. 651-659.

[14]Volpe, G. and Melnik, R. E., "The Role of Constraints in the Inverse Design Problem for Transonic Airfoils," AIAA Paper 81-1233, 1981; also *AIAA Journal* Vol. 22, 1984, pp. 1770-1778.

[15]Volpe, G., "The Inverse Design of Closed Airfoils in Transonic Flow," AIAA Paper 83-504, 1983.

[16]Volpe, G. and Melnik, R. E., "The Design of Transonic Airfoils by a Well-Posed Inverse Mehtod," Paper presented at International Conference on Inverse Design Concepts in Engineering Sciences, Austin, TX, 1984; also *International Journal for Numerical Methods in Engineering*, Vol. 22, 1986, pp. 341-361.

[17]Ludford, G. S., "The Behavior at Infinity of the Potential Function of a Two-Dimensional Subsonic Compressible Flow," *Journal of Mathematical Physics*, Vol. 30, 1951, pp. 117-130.

[18]Jameson, A., "Acceleration of Transonic Potential Flow Calculations on Arbitrary Meshes by the Multiple Grid Method," AIAA Paper 79-1458, 1979.